6-1-2000

Aseismic Inflation of Westdahl Volcano, Alaska, Revealed by Satellite Radar Interferometry

Zhong Lu
U.S. Geological Survey

Charles Wicks
U.S. Geological Survey

Daniel Dzurisin
U.S. Geological Survey

Wayne Thatcher
U.S. Geological Survey

Jeffrey T. Freymuller
Universtiy of Alaska Fairbanks

See next page for additional authors

Aseismic inflation of Westdahl volcano, Alaska, revealed by satellite radar interferometry

Zhong Lu,[1] Charles Wicks,[2] Daniel Dzurisin,[3] Wayne Thatcher,[2] Jeffrey T. Freymueller,[4] Stephen R. McNutt,[4] and Dörte Mann[4]

Abstract. Westdahl volcano, located at the west end of Unimak Island in the central Aleutian volcanic arc, Alaska, is a broad shield that produced moderate-sized eruptions in 1964, 1978-79, and 1991-92. Satellite radar interferometry detected about 17 cm of volcano-wide inflation from September 1993 to October 1998. Multiple independent interferograms reveal that the deformation rate has not been steady; more inflation occurred from 1993 to 1995 than from 1995 to 1998. Numerical modeling indicates that a source located about 9 km beneath the center of the volcano inflated by about 0.05 km^3 from 1993 to 1998. On the basis of the timing and volume of recent eruptions at Westdahl and the fact that it has been inflating for more than 5 years, the next eruption can be expected within the next several years.

1. Introduction

The current state of the art in volcano hazard monitoring and mitigation is based on two techniques that provide information over very different time scales: (1) stratigraphic studies to elucidate a volcano's long-term eruptive history (typically 10^4 - 10^6 years) and (2) monitoring shallow-seated forms of unrest, such as seismicity and ground deformation, that are typically recognized a few days to months before an eruption. Because volcanoes sometimes erupt a cubic kilometer or more of magma in a brief span of hours to days, it seems likely that large volumes of magma accumulate somewhere in the middle to lower crust during intervals between large eruptions, presumably over time scales of years to centuries. However, deep magma reservoirs are difficult to detect beneath most volcanoes, perhaps because (1) deep magma accumulation occurs below the brittle/ductile transition and consequently is virtually aseismic and (2) any associated surface deformation is relatively subtle. Detecting a deep-seated deformation signal years to decades before the onset of shallow unrest would allow scientists to focus their monitoring efforts and would permit public officials to better mitigate volcano hazards.

Satellite interferometric synthetic aperture radar (InSAR) has recently been used to study deformation at several volcanoes around the world [e.g., *Lu et al.*, 1999, 2000; *Massonnet and Feigl*, 1998; *Thatcher and Massonnet*, 1997; *Wicks et al.*, 1998] and has the capability of mapping centimeter-level deformation over large areas (~ 10^4 km^2). In this paper, we report the use of InSAR to image progressive inflation of Westdahl volcano, Alaska, during a 6-year period of quiescence following its most recent eruption in 1991-92. We also discuss how we modeled the observed surface deformation to locate the inflation source and determine its volume change since 1993.

Westdahl is a young glacier-clad shield volcano located on the west end of Unimak Island (Figure 1), in the central part of the Alaska-Aleutian volcanic arc and about 85 km southwest of the tip of the Alaska Peninsula. A thick sequence of preglacial basalt lava flows makes up most of the Westdahl edifice. The volcano was frequently active during the latter half of the 20th century, with documented eruptions in 1964, 1978-79, and 1991-92 (all Volcanic Explosivity Index 2 or 3). In 1964, a fissure eruption produced lava flows that covered 35 km^2 on the east flank of the volcano. A vulcanian eruption through glacier ice in 1978 produced a crater 1.5 km in diameter and 0.5 km deep. The November 29, 1991 eruption was reported by pilots who observed a fissure eruption through the ice. This most recent eruption eventually produced a 5~10-m-thick, 3-km-wide, 7-km-long lava flow down the volcano's northeast flank and debris flows that reached the sea 18 km from the vent. Although there was no local network at the time, seismic stations 170 km to the ENE showed 6 events with magnitude (M) ~ 3 on November 29. These events had S- and P-wave travel time difference of 17 s, consistent with locations on Westdahl. This level of seismic activity is consistent with many other swarms accompanying eruptions of similar size and type [*Benoit and McNutt*, 1996].

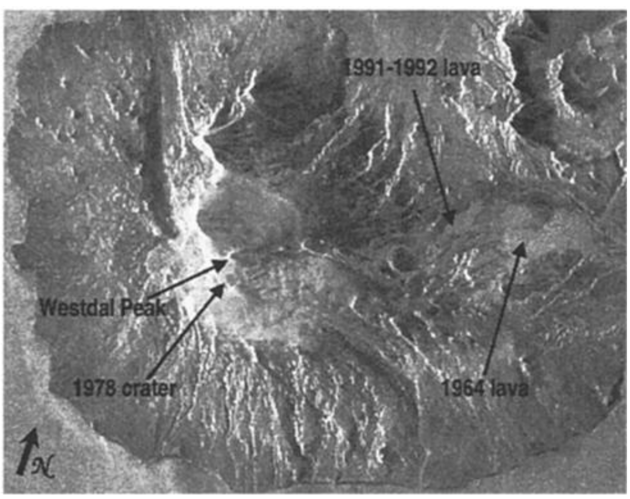

Figure 1. ERS-1 SAR image (center latitude/longitude: 54.5°N/164.6°W) of Westdahl volcano, Alaska.

[1]Raytheon STX Corporation, U.S. Geological Survey, EROS Data Center, Sioux Falls, South Dakota
[2]U.S. Geological Survey, Menlo Park, California
[3]U.S. Geological Survey, David A. Johnston Cascades Volcano Observatory, Vancouver, Washington
[4]Alaska Volcano Observatory, Geophysical Institute, University of Alaska, Fairbanks

Paper number 1999GL011283.
0094-8276/00/1999GL011283$05.00

The Alaska Volcano Observatory (AVO) deployed a five-station seismic network at Westdahl in July 1998. Since then, the background level of seismic activity has been low (~ 5 $M < 3$ earthquakes per year) and no unusual activity has been detected

2. Surface Deformation From 1992 to 1998

We selected several pairs of ERS-1 and ERS-2 images that are suitable for measuring surface deformation at Westdahl from 1992 to 1998. The summit area of the volcano is covered by glaciers that make InSAR analysis over periods of several years impossible. To minimize the amount of snow and ice cover on the flanks, we chose only images that were acquired during late summer or early autumn. Because we were in search of deformation that might be subtle and slow, we included the largest possible temporal separation. The earliest ERS data are from 1992, and 1999 data are not yet available to us. To generate deformation interferograms, we processed radar signal data obtained from the Alaska SAR Facility (ASF), together with a U.S. Geological Survey (USGS) digital elevation model (DEM) having a horizontal resolution of about 60 meters and a root-mean-square vertical error of 15 meters; for this processing, we used the two-pass InSAR method described by *Massonnet and Feigl* [1998].

Deformation interferograms of Westdahl for several periods are shown in Figure 2. In each case, the topographic contribution to the original interferogram was removed using the USGS DEM. Coherence is maintained for up to 5 years if the images are acquired during summer to late fall, except on the ice-covered upper slopes of the Westdahl edifice. In the permanently ice-covered areas, there was no radar coherence and no useful deformation signals could be extracted (i.e., uncolored regions in Figure 2), even over 3-day time intervals. The fringe patterns in Figure 2 cannot be caused by atmospheric delays, for two reasons: (1) the overall deformation pattern is consistent from 1992 to 1998, whereas atmospheric delays are ephemeral; and (2) essentially the same fringe pattern is seen with independent image pairs from both descending and ascending satellite passes. Neither can the observed inflation pattern be caused by plausible errors in the DEM, because the baselines (spatial distance between two satellite trajectories) of image pairs for the 1993-98 and 1992-97 interferograms are only 23 m and 12 m, respectively. With such short baselines, possible errors in the DEM would contribute no more than one-tenth of one fringe to the interferograms.

The 1993-98 deformation interferogram is shown in Figure 2a. The images used for the interferogram were acquired in descending mode while the ERS satellites traveled from north to south and looked to the west. At least two concentric fringes can be seen around most of the volcano (about three full fringes appear on the southwest flank). Each fringe represents 2.83 cm of range change along the satellite look direction. Because the look angle for the ERS satellites is only 23° from vertical, the interferograms are mostly sensitive to vertical motion, in this case uplift centered near the volcano's summit (where glaciers destroy radar coherence). The 1993-98 deformation does not extend all the way to the northwestern tip of the island, but areas more than 10 km from the summit are clearly affected. The breadth of the deformation field implies that its source is more than a few kilometers deep, and its shape and position indicate that the source is relatively symmetric and located beneath the summit area.

The 1992-97 interferogram (Figure 2b) suffers from a larger area of incoherent signals on the volcano's upper flanks, but one to one-and-a-half circular fringes are clearly visible. The images used to produce this interferogram were acquired in October 1992 and June 1997 while the satellites were in ascending mode, moving from south to north and looking to the east. The northwesternmost part of the island, where little or no deformation was revealed by the 1993-98 interferogram, is out of the imaging swath for both the 1992-97 and 1993-96 interferograms (Figures 2b and 2c). The 1993-96 fringe pattern, which was generated from images acquired in descending mode, is similar to the 1993-98 pattern except that fractionally fewer fringes are visible over the shorter interval and the area of coherence loss is smaller than that of the 1993-98 interferogram.

3. Location and Volume Change of the Magma Body

To estimate the location and volume change of the inflation source responsible for the surface deformation at Westdahl, we modeled the interferograms in Figures 2a to 2e using a point source embedded in an elastic homogeneous half-space [*Mogi*, 1958]. We interpret this source to represent a magma chamber at depth. The four parameters used to describe the source are horizontal location (x and y coordinates), depth, and strength, which is related to a change in pressure, volume, or both. Initially, we placed the source directly beneath the summit of the volcano at a depth equal to the radius of the most distant fringe (~10 km). A nonlinear least squares inversion approach was used to optimize the source parameters [*Press et al.*, 1992]. This approach minimizes a merit function defined as the chi-squared difference between the observed and synthetic interferograms. The Levenberg-Marquardt Method [*Press et al.*, 1992] was used to iteratively improve the trial solution until the chi-squared difference effectively stopped decreasing.

Before modeling, we "unwrapped" each of the interferograms shown in Figure 2, using the technique described by *Goldstein et al.* [1988]. In areas with good coherence and clearly differentiated fringes, repetitive phase values ranging from 0 to 2π can be unwrapped to produce a cumulative displacement field. We carefully examined the unwrapped interferograms to ensure that no artifacts were created during the unwrapping process, then inverted the unwrapped interferograms to determine best fit source parameters for each case.

The best fit synthetic and residual (observed minus synthetic) interferograms for the 1993-98 case are shown in Figure 3. The inferred source is located almost directly beneath the summit of Westdahl volcano at a depth of 8.7 km. The horizontal and vertical uncertainties are ±1.5 km and ±0.8 km, respectively. The best fit model suggests that this source inflated by 0.05 km^3 from 1993 to 1998, causing an inferred maximum surface uplift of 16.6 cm above the source. This corresponds to an average uplift rate of the summit of ~3 cm/yr, or approximately one fringe/yr. More than half of the deformation would have been localized in the ice-covered summit region where the radar images were not coherent, because the model produces almost six fringes for the 1993-98 interval but only two to three were observed. Modeling of

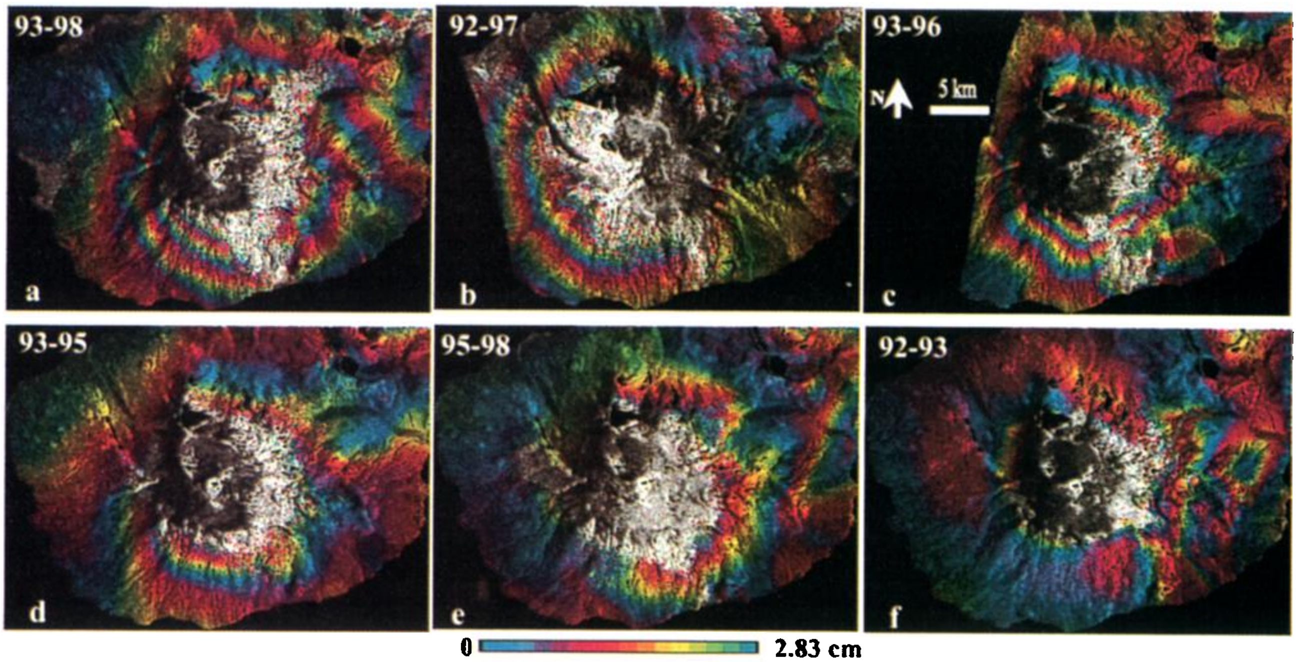

Figure 2. Deformation interferograms of the Westdahl volcano spanning the time intervals (a) from September 21, 1993, to October 9, 1998, (b) from October 11, 1992, to June 11, 1997 (c)from October 7, 1993, to August 11, 1996, (d) from September 21, 1993, to October 19, 1995, (e) from October 19, 1995, to October 9, 1998, and (f) from October 6, 1992, to September 21, 1993. Areas of loss of radar coherence are uncolored. Each image is 40.0 km wide (E-W) by 28.8 km long (N-S).

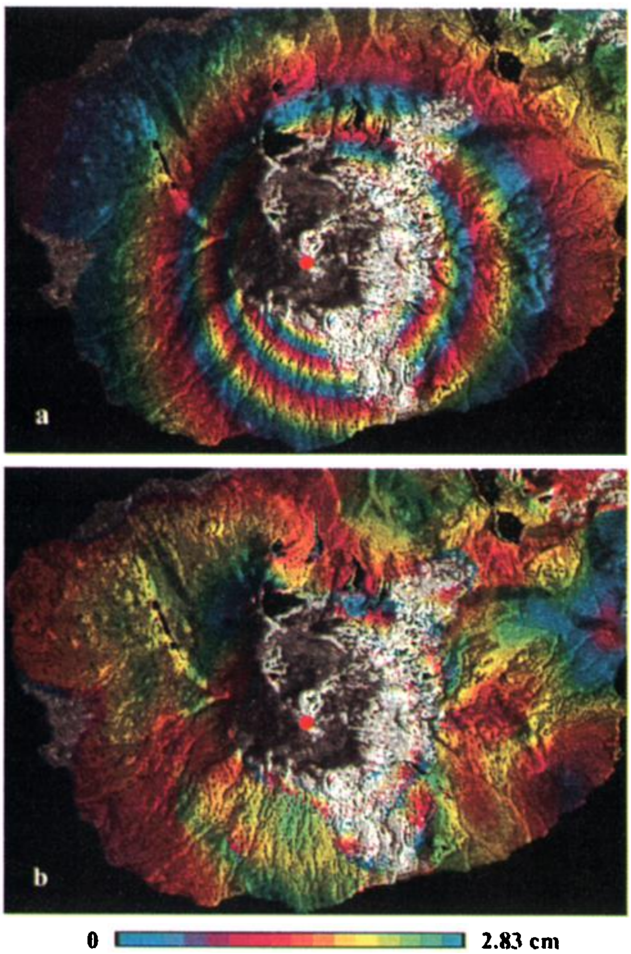

Figure 3. (a) Synthesized interferogram with best fitting model for 1993-98 interferogram (Figure 2a). (b) Residual interferogram indicating the difference between the observed and modeled interferograms (Figures 2a and 3a). The red dot at image center represents location of the best fitting source.

the other interferograms in Figures 2b to 2e produced similar results.

4. Discussion

Relatively short-wavelength, ephemeral fringe patterns (<2.0 cm in magnitude) appear on the east flank of Westdahl volcano in most of the residual interferograms (see, for example, the region in the lower right of Figure 2f). These unmodeled fringes are most likely caused by atmospheric delay anomalies [*Lu et al.*, 2000; *Zebker et al.*, 1997]. However, the main fringe pattern is consistent through all of the time periods.

The 1993-95, 1995-98, and 1993-98 interferograms (Figs. 2d, 2e, and 2a, respectively) were produced from a total of three images, so each interferogram shares an image with another. When time differences are taken into account, the fringe patterns in all three interferograms are similar, even though the first two cases include just one fringe each and are therefore unconvincing on their own. To check for consistency, we summed the 1993-95 and 1995-98 interferograms and compared the result with the observed 1993-98 interferogram. The two interferograms generally agreed with one another to within 3 mm, suggesting that the fringe patterns for 1993-95 and 1995-98 represent real ground deformation and not atmospheric delay anomalies.

Using this assumption, we compared the 1993-95 and 1995-98 interferograms and found that the inflation rate seems to vary with time. More than one fringe was observed for the 2-year interval from 1993 to 1995, but no more than one complete fringe was observed for the 3-year interval from 1995 to 1998. This suggests that inflation has slowed over time since the 1991-92 eruption. InSAR studies spanning the 1997 eruption of Okmok volcano, Alaska, show that the preeruptive inflation rate also varied [*Lu et al.*, 2000]. Those studies found that the inflation rate from 1992 to 1993 was about twice that from 1993 to 1995. Observations at Kilauea volcano, Hawaii, suggest that the inflation rate of some volcanoes may be highest immediately after eruptions, when the depleted magma reservoir is rapidly replenished from depth, and becomes progressively lower as the next eruption approaches [*Dvorak and Dzurisin*, 1997]. Results from Westdahl and Okmok suggest that similar behavior might hold for volcanoes in a very different tectonic setting. Repeated InSAR and Global Positioning System (GPS) measurements at Okmok and Westdahl should be sufficient to test whether this observation holds for an entire eruptive cycle (one to two decades).

An alternative explanation of the 1993-95 and 1995-98 interferograms at Westdahl is that the inflation source was shallower during the latter period, in which case the inflation rate might have remained constant or even increased. A shallower source would produce more localized deformation on the upper flanks of the volcano, where deformation is masked by coherence loss. If the deformation source is becoming shallower, continued inflation should eventually produce earthquakes in the upper, brittle part of the crust beneath Westdahl; earthquakes have not yet been observed in the short interval since the installation of the local seismic network. We thus prefer the interpretation that inflation of a fixed, 8-km-deep magma reservoir has slowed somewhat since 1995. GPS measurements were begun in 1998 and surveyed in 1999. We plan to compare the GPS results with InSAR observations for 1998-99 when 1999 SAR data are available.

There may be a precedent for a change in source depth between periods of inflation and deflation at the same volcano. *Lanari et al.* [1998] produced sequential interferograms for Mount Etna that reveal deflation near the end of the 1991-93 eruption, inflation before the 1995 eruption, and quiescence for a year thereafter. A point-source, elastic model suggests that the deformation source might have changed depth, from 9 km during deflation to 11-14 km during the subsequent inflation, although it is possible that the uncertainties in the depth estimates may be too large to rule out a single depth for both inflation and deflation sources. This result seems reasonable if the magma chamber is a vertically extended region that empties from the top during eruptions and fills from the bottom between eruptions.

Deformation at Westdahl volcano extends more than 10 km from the summit in all directions. Few geodetic networks at volcanoes are this large, and therefore most are inadequate to detect or fully characterize deformation sources deeper than a few kilometers. InSAR seems to be the best tool available for detecting deep, aseismic magma accumulation by measuring broad, subtle deformation of the ground surface. Especially if combined with GPS or borehole strain measurements, repeated InSAR observations could help to identify restless volcanoes long before they become active. The warning time before eruptions might be extended to years or even decades, filling a crucial gap between traditional volcano monitoring of shallow precursors (hours to months of warning) and long-term volcano hazards assessments based on a volcano's eruptive history (decades to centuries). The additional lead time would allow scientists to focus their monitoring efforts more closely on particularly hazardous volcanoes and would provide public officials an opportunity to further mitigate losses through informed land use decisions together with shorter term emergency response plans.

Acknowledgments. ERS-1 and ERS-2 SAR data are copyrighted 1992, 1993, 1995, 1996, 1997, and 1998 by ESA. We thank the ASF for providing the SAR data, J. Power for helpful discussions on seismicity, and M. Choate, T. DeFelice, and S. Liu for USGS internal reviews. Comments by M. Murakami and an anonymous reviewer improved the manuscript quality. Lu was supported by USGS contract 1434-CR-97-CN-40274. Wicks, Dzurisin, and Thatcher were supported by the USGS Volcano Hazards Program. Freymueller, McNutt, and Mann were partially supported by the AVO, and supported by NASA contract NAG5-7659.

References

Benoit, J.P. and S.R. McNutt, Global volcanic earthquake swarm database 1979-1989, *U.S. Geolo. Surv. Open File Rep., 96-69*, 1996.

Dvorak, J., and D. Dzurisin, Volcano geodesy: the search for magma reservoirs and the formation of eruptive vents, *Rev. Geophys., 35*, 343-384, 1997.

Goldstein, R., H. Zebker, and C. Werner, Satellite radar interferometry: Two-dimensional phase unwrapping, *Radio Sci., 23*, 713-720, 1988.

Lanari, R., P. Lundgren, E. Sansosti, Dynamic deformation of Etna volcano observed by satellite radar interferometry, *Geophys. Res. Lett., 25*, 1541-1544, 1998.

Lu, Z., D. Mann, J. Freymueller, and D. Meyer, Synthetic aperture radar interferometry of Okmok volcano, Alaska: Radar observations, *J. Geophys. Res.*, in press, 2000.

Lu, Z., C. Wicks, J. Power, and D. Dzurisin, Deformation of Akutan volcano, Alaska, revealed by satellite radar interferometry, *J. Geophys. Res.*, submitted 1999.

Massonnet, D., and K. Feigl, Radar interferometry and its application to changes in the Earth's surface, *Rev. Geophys., 36*, 441-500, 1998.

Mogi, K., Relations between the eruptions of various volcanoes and the deformations of the ground surface around them, *Bull. Earthquake Res. Inst. Univ. Tokyo, 36*, 99-134, 1958.

Press, W., S. Teukolsky, W. Vetterling, and B. Flannery, Numerical recipes in C, the art of scientific computing, Cambridge Univ. Press, 994 pp., 1992.

Thatcher, W., and D. Massonnet, Crustal deformation at Long Valley Caldera, eastern California, 1992-1996, inferred from satellite radar interferometry, *Geophys. Res. Lett., 24*, 2519-2522, 1997.

Wicks, C., W. Thatcher, and D. Dzurisin, Migration of fluids beneath Yellowstone Caldera inferred from satellite radar interferometry, *Science, 282*, 458-462, 1998.

Zebker, H., P. Rosen, and S. Hensley, Atmospheric effects in interferometric synthetic aperture radar surface deformation and topographic maps, *J. Geophys. Res., 102*, 7547-7563, 1997.

D. Dzurisin, USGS, Cascades Volcano Observatory, 5400 MacArthur Blvd., Vancouver, WA 98661

J.T. Freymueller, D. Mann, and S.R. McNutt, AVO, Geophysical Institute, University of Alaska Fairbanks, Fairbanks, AK 99775

Z. Lu, Raytheon STX Corporation, USGS/EROS Data Center, Sioux Falls, SD 57198 (lu@edcmail.cr.usgs.gov)

W. Thatcher, and C. Wicks, USGS, 345 Middlefield Rd. MS 977, Menlo Park, CA 94025-3591

(Received December 15, 1999; revised February 16, 2000; accepted March 8, 2000.)